Progress In Electromagnetics Research C, Vol. 113, 111–122, 2021

Eight-Port Double Band Printed MIMO Antenna Investigated for Mutual-Coupling and SAR Effects for Sub-6 GHz 5G Mobile Applications

Insha Ishteyaq*, Issmat S. Masoodi, and Khalid Muzaffar

Abstract—An 8-element/8-port antenna with four resonating dual-polarized slot radiator elements for sub-6 GHz 5G multiple-input multiple-output (MIMO) applications is proposed in this paper. The proposed MIMO design comprises four annular slot radiators with dual-polarized characteristic and has rectangular micro-strip line feeds. The designed elements operate in the frequency bands 2.73–3.12 GHz and 4.33–4.68 GHz providing an acceptable characteristic for dual-polarizations. The isolation improvement and reduction in mutual coupling factor are achieved by using split ring resonator (SRR) structures on the top layer along the slot radiator. The proposed design has a -10 dB wide impedance bandwidth in both bands, considerable realized peak gain around 4 dBi, and better efficiencies around 80% with ECC < 0.004 which has enhanced the performance of the MIMO array in terms of diversity. The antenna is fabricated, characterized, and it is shown that the measured results are in good agreement with the simulated ones. The proposed MIMO design has been analyzed for SAR functions and the radiation coverage in the vicinity of the user human head. The SAR values studied are found to be less than '2' which is quite desirable. All the features achieved in the proposed MIMO design suggest it to be suitable for 5G mobile terminal applications.

1. INTRODUCTION

The fifth generation (5G) technologies with incredible speeds are the emerging communication systems targeted to be deployed in 2020 [1]. It is certain that the thriving 5G indoor access microwave wireless devices and 5G wireless routers need to be employed to connect Internet of things in the near future [2]. For 5G communications, 5G antennas will become a necessity to be used along both sides of a communication link in order to achieve higher data rate transmission and short latency in comparison to already existing 4G systems [3]. In order to improve the various constraint parameters including data rates, channel capacity, reliability, etc. for 5G service in multi-path domain MIMO technology has proved to be highly productive [4]. The design of proficient MIMO antenna system requires the antennas with low profile, easy fabrication, and high isolation between antenna elements [5–7].

The international telecommunication union (ITU) has declared sub-6 GHz and mm-wave spectrum for 5G MIMO applications for mobile antenna terminals, mainly including 3.4–3.8 GHz, 3.7–4.2 GHz, 5–6 GHz, 24–28 GHz, etc. frequency bands [8]. For 5G MIMO applications, the sub-6 GHz frequency bands are proved to be more suitable and mainly include n77(3.3–4.2 GHz), n78(3.3–3.8 GHz), n79(4.4–5 GHz), 3.3–3.8 GHz, and 5.15–5.925 GHz that represent a combination of LTE 42, 43, 46 bands [9, 10]. A slot antenna with multi-band operation at 1.5 GHz, 2.75 GHz, and 3.16 GHz with around 3 dB gain and efficiency of 80% is presented in [11], and a wide-band horn antenna with ridged substrate integrated with waveguide (RSIW) structure is given in [12]. The number of techniques for reducing the coupling effects

Received 3 May 2021, Accepted 7 June 2021, Scheduled 13 June 2021

* Corresponding author: Insha Ishteyaq (insha.ishteyaq@islamicuniversity.edu.in).
The authors are with the Islamic University of Science and Technology, Awantipora, Jammu and Kashmir, India.

among the different antenna elements in MIMO systems has been reported which mainly include the use of decoupling mechanism depending on isolating elements [13], antennas placed asymmetrically [14], metal shorting strips or grounding stubs [15], defected ground structures [16], neutralization lines between elements [17], and ground strips between antenna elements [18]. Nowadays, co-design of 4G and 5G antennas is becoming an important area of research [7].

With the widespread application of mobile devices in the present scenario, a serious concern related to the human health has arisen. The effect is posed due to hazardous effects of the electromagnetic waves utilized by the mobile phones while they receive or transmit data. The electromagnetic (EM) radiations can have temporary as well as permanent effects on the health of human leading to most severe diseases in many cases [19]. The studies show that the human tissues convert the em energy into heat which in turn causes the rise of temperature or thermal effects in the body. The parametric factor that is used to evaluate this energy absorption is specific absorption rate (SAR). It is the dissipated energy by a mass/volume of tissue with the given density [20]. As per IEEE SAR is defined as, SAR $= \sigma E^2/\rho$ where ρ refers to the density of human tissue. σ refers to the conductivity of human tissue.

A MIMO array antenna with 8-PIFA (planar inverted F antenna) elements is presented for 5G mobile applications along with good isolation and very low SAR effects [21]. The diversity MIMO antenna having coplanar waveguide (CPW) fed T-slot radiators offering good isolation minimum impact of SAR is presented in [22]. An antenna array for both 4G and 5G applications having good user performance and low SAR effects in the presence of biological tissues is presented in [23]. A MIMO array having slots of diamond ring shape with high efficiency and good isolation between antenna elements is investigated for 5G applications [24]. The design presents effects with respect to user working in talk mode and has shown much better results. An antenna with a rectangular slot for double band operation is presented for sub-6 GHz 5G applications. The antenna is verified for back cover effects of a mobile terminal as well as for user impact in addition to SAR effects [25]. An E-shaped wearable and flexible dipole antenna for multiband applications with extremely safer value of resulting SAR is shown in [26].

In this paper, a MIMO antenna array with 8-elements and orthogonally polarized annular slot elements is presented for sub-6 GHz 5G applications. The antenna element is fed by a micro-strip rectangular line, and the square split ring resonators (SRRs) are used across the annular slot in order to develop the high isolation between the feeding ports. The annular ring slots act as main radiators and are placed all along the corners of the mobile PCB to enhance the coverage due to different polarizations. The proposed MIMO design and its single antenna element are simulated and fabricated. The prototype of the MIMO antenna is characterized for all the parameters depicting all the results that seem good enough for MIMO applications. The radiation pattern and S-parameters are studied in addition to envelop correlation coefficient (ECC) and diversity gain to appraise multiplexing and diversity performances. SAR parameter is also studied keeping in consideration the safety of the users handling the mobile device. The paper is organized as follows. Section 2 describes the overall design of the proposed MIMO antenna explaining the principle and characterization of 2-element [2.1] and 8-element [2.2] antenna designs. The impact of EM waves on the users and SAR effects are described in Section 2.3, and the paper is concluded in Section 3.

2. ANTENNA DESIGN

2.1. 2-Element MIMO Antenna

The antenna single element comprises an annular ring shaped slot b etched on the bottom ground surface which acts as the main radiator and is fed by micro-strip lines placed perpendicularly on the top corners of the FR4 substrate. On the top side, two SRRs are placed at optimized locations across the circular slot. The antenna is designed on both sides of an FR4 substrate with a loss tangent ($\delta = 0.025$) and relative permittivity ($\epsilon_r = 4.3$) having thickness '$h = 1.6$ mm'.

The configuration of the proposed 2-port MIMO design is shown in Fig. 1 with all the dimensions (in 'mm') of the single antenna element. The single antenna element can be treated as a 2×2 MIMO antenna which is fed by orthogonally placed micro-strip lines at the corner of PCB making the antenna dual polarized. The proposed antenna element is simulated using CST Microwave Studio Suite to evaluate all the characteristics including S-parameters, gain, efficiencies, ECC, diversity gain (DG), etc. One of the important constraint factor in MIMO design is high mutual coupling between antenna

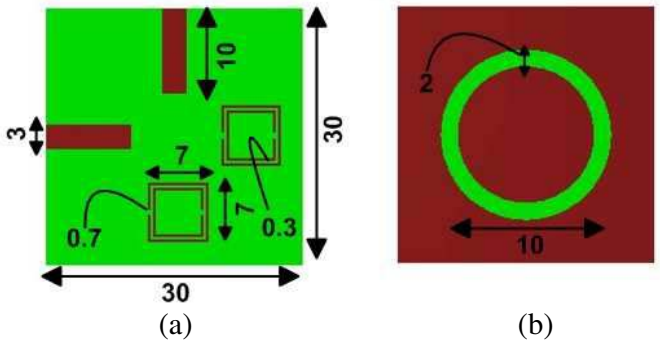

Figure 1. Schematic of the single element antenna, (a) top view, (b) bottom view.

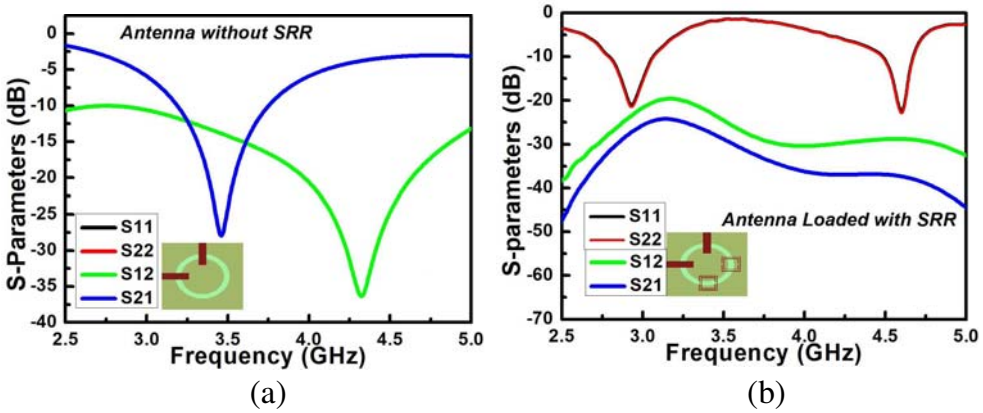

Figure 2. S-parameters of the 2×2 single MIMO element, (a) without SRR, (b) with SRR.

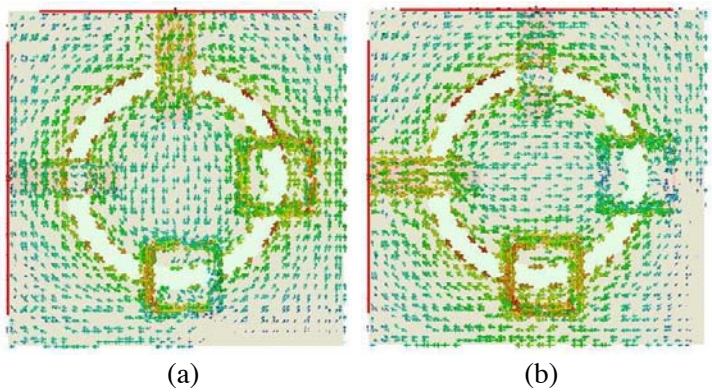

Figure 3. Surface current distribution of the 2×2 single MIMO element, (a) when fed from port-1, (b) when fed from port-2.

elements due to restricted amount of space inside mobile antenna terminals. It becomes a necessity to acquire large isolation among the elements of a MIMO design [27]. In the proposed design, SRRs are employed for reducing the mutual coupling among the elements of the MIMO antenna. The loading of SRR has improved the isolation to a great extent, i.e., from -12.36 dB to around -22.5 dB as shown in Fig. 2.

The surface current sharing of the double polarized annular slotted antenna is depicted in Fig. 3

at 3 GHz frequency. As observed from the figure, major currents are directed along the etched annular ring slot from the ground plane. The double polarized parameter is produced by the currents flowing antithetically to one another for the separate port feeds. The SRR structures have been shown to have dense current distributions with respect to feeding ports 1 and 2 which have eventually reduced the mutual coupling among the antenna elements. The SRR structures placed on the top of substrate across the annular slot ring (ASR) are aimed at reducing the mutual coupling between the antenna elements. For separating feeding ports, the currents are distributed along the orthogonally placed SRR with respect to feed element. The SRR structures tend to increase the current density along its boundaries for respective ports thereby minimizing the coupling currents between them. The surface currents are mainly concentrated along the boundaries of SRR, and it is also observed that the currents are flowing in opposite directions for separate feeding ports because of effect of SRR elements. The overall current distributions tend to align the currents actively for the ports in turn enhancing the isolation among the antenna elements. It can be deduced that the employed SRR structures have high current densities and emerge highly active at the operating frequency of the proposed MIMO design. The resonant structures are employed actively at the respective working frequency bands of 2.73–3.12 GHz and 4.32–4.68 GHz for the improvement of isolation in the MIMO design.

The frequency response of the proposed design and the mutual coupling parameter are largely dependent on the position of the SRR structures. The characteristics of the MIMO antenna for different locations of the SRR with respect to the feed and annular slot radiator are studied and optimized for better results. It has been observed that the orthogonal placement is the best option wherein high isolation as well as stable characteristics for S_{11} & S_{22} for the desired operating frequency band is achieved. Thus, the position of the SRR elements in relation to feeding lines and ASR pose a significant impact on the characteristics of the MIMO antenna mainly in terms of mutual coupling and stable operating frequency range.

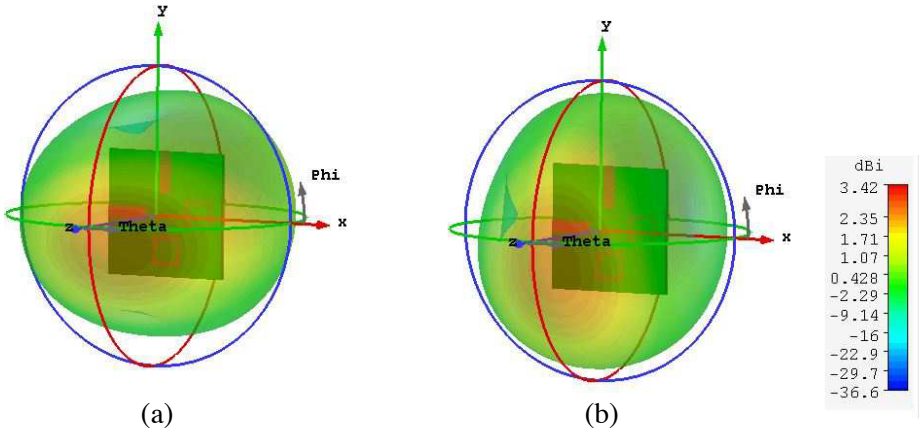

Figure 4. Three dimensional patterns of the 2 × 2 single MIMO element showing dumb-bell shaped pattern representing the radiation coverage on both sides of the slot radiator, (a) when fed from port-1, (b) when fed from port-2.

The three-dimensional views of the radiation patterns of 2-element MIMO at 3 GHz and 4.5 GHz for the two respective ports are shown in Fig. 4. It is observed that for two separate polarizations, the radiating characteristics are same along with the directivity around 3.42 dBi. The slot antenna seems to produce a dumb-bell shaped pattern which is desirable for the better coverage from both top and bottom of the mobile PCB mainly for MIMO 5G applications.

2.2. Proposed MIMO Design for 5G Application

The schematic of the proposed MIMO antenna design is shown in Fig. 5. The proposed design is configured on both sides of an FR4 substrate having loss-tangent and relative permittivity of 4.4 and 0.025, respectively. The design possesses the total dimension of $150 \times 70\,\text{mm}^2$ with annular slot elements

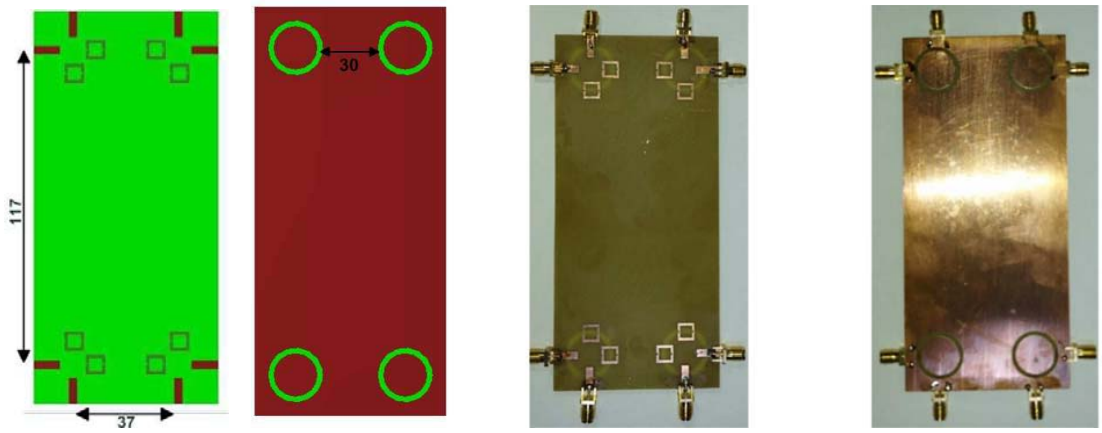

Figure 5. Schematic and the fabricated prototype of the proposed MIMO design having slot radiators and loaded with SRR structures for isolation improvement, (i) top view of schematic, (ii) bottom view of schematic, (iii) top view of prototype, (iv) bottom view of prototype.

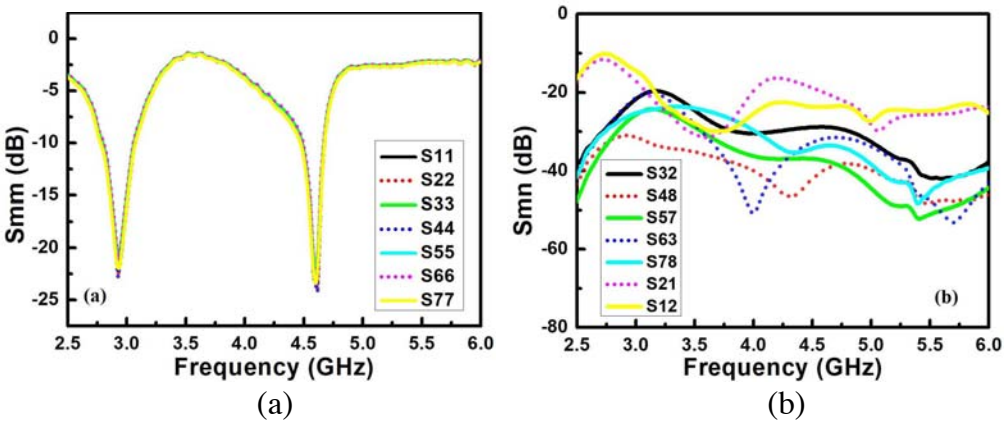

Figure 6. Simulated results for S-parameters of the proposed 8-element MIMO design, (a) reflection coefficient (S_{mm}), (b) mutual coupling S_{mn}.

having outer and inner radii of 10 mm and 8 mm, respectively, placed along the four corners of the PCB smart phone. Fig. 6 shows the simulated S-parameters which include the characteristics of both reflection coefficient (S_{nn}) and mutual coupling (S_{mn}) of the double-polarized proposed MIMO design.

The simulated results depict the under -10 dB impedance bandwidth in the two operating frequency bands with the isolation under -20 dB in the resulting bands. The isolation is achieved by loading the antenna with split ring resonators perpendicularly across the annular slots. The resonator structures have diversified the surface currents, i.e., while feeding from any of the ports the corresponding SRR makes the maximum current flow through itself preventing it to reach the second antenna element. The resulting pattern of the current density flow has reduced the mutual coupling between the elements to a greater extent thus improving isolation to less than than -20 dB. The resulting band satisfies the criteria for 5G applications for Sub-6 GHz 5G MIMO applications as stated by ITU.

The proposed 5G MIMO antenna configuration with the annular slot radiators exhibits satisfying impedance bandwidth along with the symmetric patterns in order to accomplish all the sides of PCB mobile terminal. The 3-D top view of radiation patterns of the proposed dual-polarized antenna elements is shown in Fig. 7. The radiation patterns seem to cover all the terminal edges along with top and bottom portions of the mobile PCB.

The proposed design is fabricated on top and bottom of the epoxy FR-4 substrate as shown in

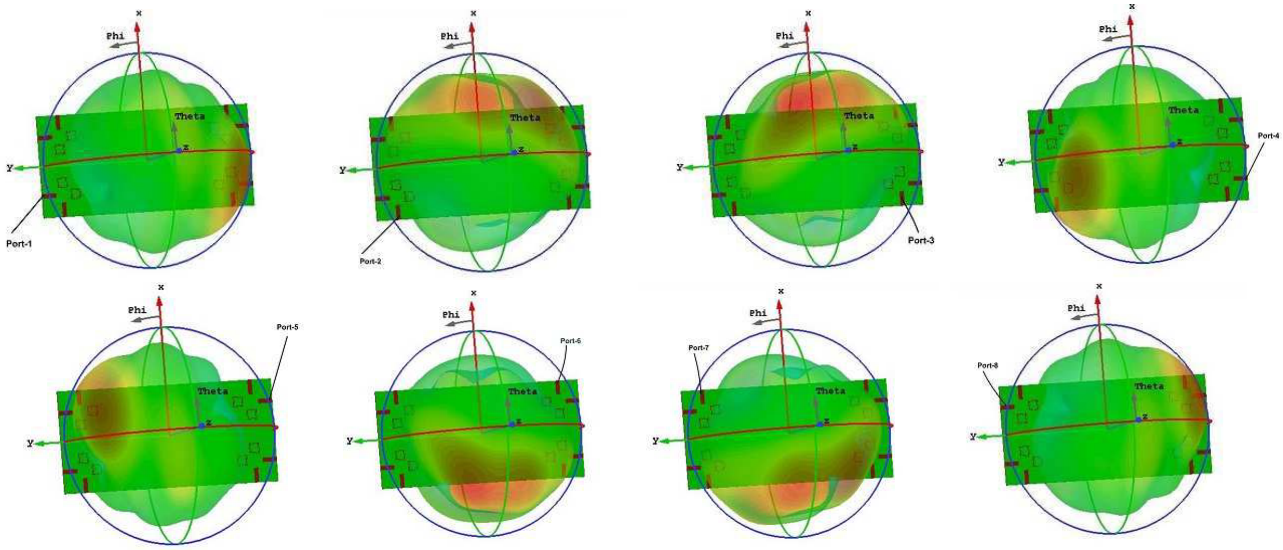

Figure 7. Radiation patterns (3-D view) of the individual antenna elements covering top and bottom from all sides of mobile terminals with respect to excited ports at the frequency of 3 GHz & 4.5 GHz.

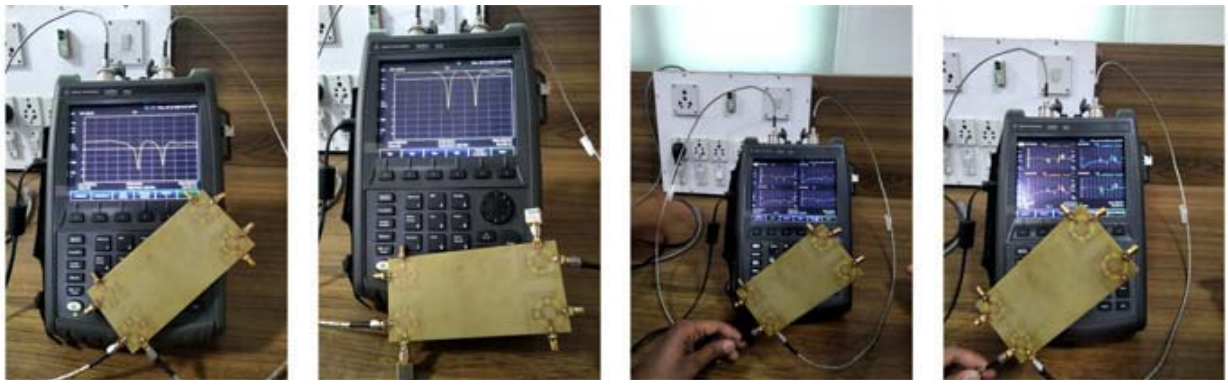

Figure 8. Characterization of the proposed fabricated MIMO antenna design using RF network analyzer and standard anechoic chamber set-up.

Fig. 5 by employing the conventional process of photo-etching. The anechoic measurement setup with a standard horn antenna along with Agilent technologies RF-network analyzer has been used to characterize the proposed MIMO design as shown in Fig. 8. The simulated and measured results for reflection coefficient and mutual coupling are shown in Fig. 9. Its evident from the figure that simulated and measured results are in good agreement with each other in the operating bands of 2.73–3.12 GHz and 4.32–4.68 GHz.

It is interpreted from Fig. 10 that the simulated and measured total efficiencies and the peak realized gains of the proposed MIMO design are in good agreement. The realized efficiency of the overall MIMO design is more than 80%. The measured peak gain of the proposed MIMO design is around 4 dBi in the resulting bands of 2.73–3.12 GHz and 4.32–4.68 GHz.

For the perfect matching of the antenna and its feed lines, the numerical value of voltage standing wave ratio (VSWR) needs to be below '2' which is quite suitable for the antenna applications. The most important parameter which describes the pattern diversity realization of the MIMO antenna arrays is ECC. Smaller values of ECC refers to the more diversified radiation patterns [28], and as a rule it must be less than 0.5 for desired MIMO design systems. Parameter ECC is also an effective term

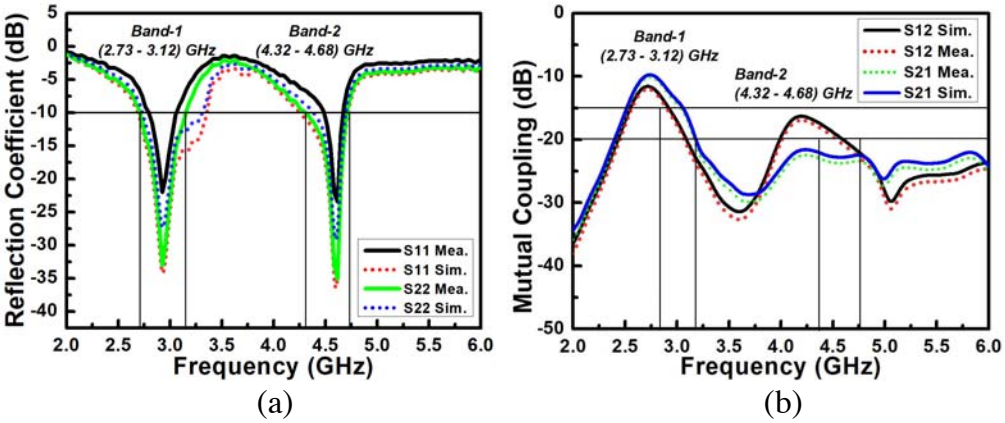

Figure 9. Simulated and measured results for the proposed MIMO antenna, (a) reflection coefficient, (b) mutual coupling.

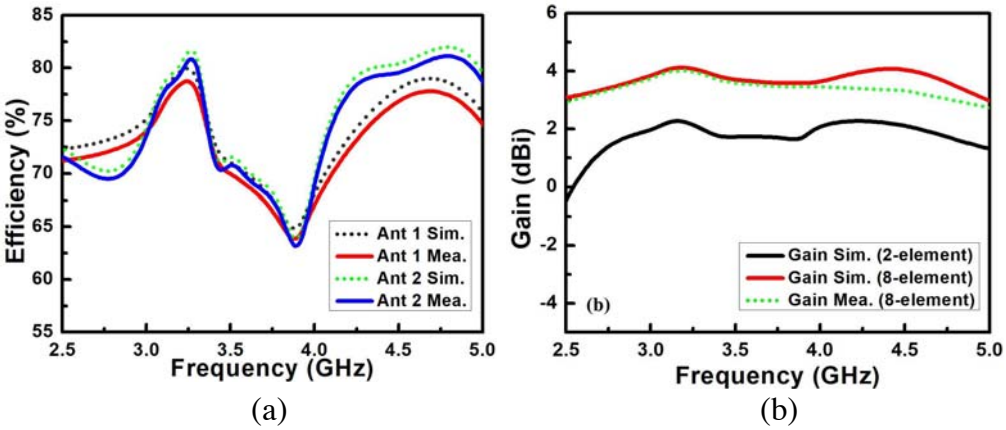

Figure 10. Simulated and measured results for, (a) efficiencies of different antenna elements, (b) realized gain of the MIMO design.

in determining the isolation between the antenna elements. ECC is an important parameter used to signify the extent of coupling between the elements. It can be determined by calculating S-parameters which include reflection coefficient as well as mutual coupling parameters. Mathematically, ECC can be calculated as [21]:

$$\text{ECC} = \frac{\left|S_{11}^{*}S_{12} + S_{21}^{*}S_{22}\right|^{2}}{\left[1-\left(|S_{11}|^{2}+|S_{21}|^{2}\right)\right]\left[1-\left(|S_{22}|^{2}+|S_{12}|^{2}\right)\right]}$$

In the case of radiating elements, the correlation is susceptible to the intrinsic losses. However, the S-parametric method for calculating ECC does not take into account these losses. The method becomes unrealistic for the antenna designs having efficiency less than 100%. To overcome the limitation of this method, the ECC can be calculated by using the EM integral equation taking into account the far-field patterns. The integral EM wave equation for ECC is shown as follows [29]:

$$\rho_e = \left| \frac{\displaystyle\int_0^{2\pi}\int_0^{\pi}\left(XPRE_\theta iE_\theta j^{\star}P_\theta + XPRE_\phi iE_\phi j^{\star}P_\phi\right)\sin\theta d\theta d\phi}{\displaystyle\prod_k = i,j \int_0^{2\pi}\int_0^{\pi}\left(XPRE_\theta kE_\theta k^{\star}P_\theta + XPRE_\phi kE_\phi k^{\star}P_\phi\right)\sin\theta d\theta d\phi} \right|^2$$

where $E_\theta i,\ E_\phi i,\ E_\theta j,\ E_\phi j$ represent the far-field components for ports i & j. P_θ and P_ϕ are the elevation

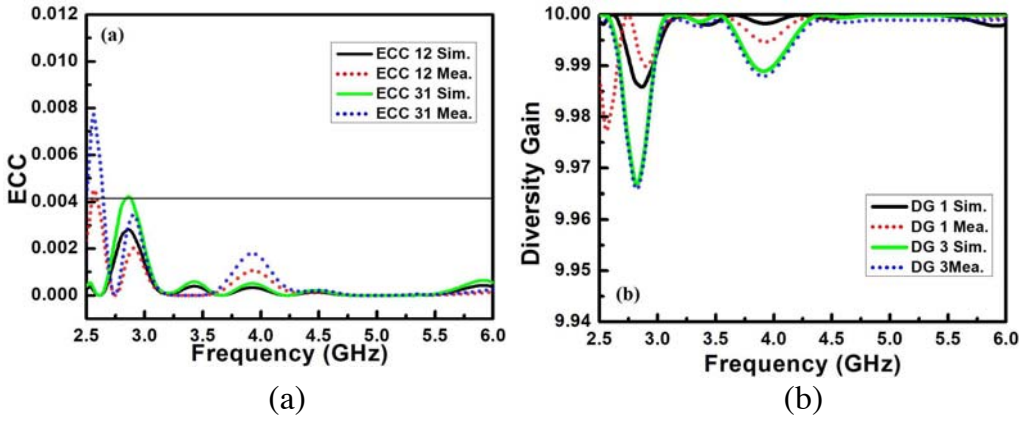

Figure 11. Simulated and measured results for, (a) ECC between antenna elements, (b) diversity gain of MIMO elements.

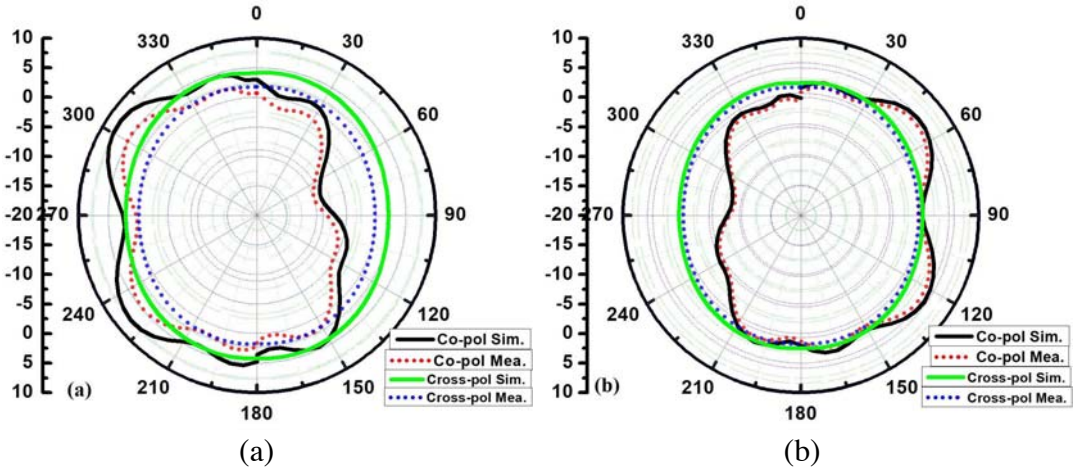

Figure 12. Simulated and measured polar patterns of the adjacent antenna elements at 3 GHz frequency.

and azimuth APS distributions, and $XPR = \frac{P_V}{P_H}$ is the cross discrimination ratio.

The ECC of the proposed MIMO design is around 0.0001 which depicts that the antenna elements are very meagerly coupled to each other. The less value of ECC has resulted in extremely reliable isolation or reduced mutual coupling. It is depicted in Fig. 11(a) that ECC of the proposed design is well below 0.004, and Fig. 11(b) depicts that the diversity gain of the proposed MIMO design is nearly 10 for both operating frequency bands which makes the proposed antenna design very efficient with regard to sub-6 GHz 5G MIMO applications.

All the resulting parameters which include reflection coefficient ($S_{nn} < -10$ dB) of (2.73–3.12) GHz and (4.32–4.68) GHz are applicable to 5G sub-6 GHz MIMO applications and mutual coupling ($S_{mn} < -20$ dB) for good isolation between the antenna elements. ECC < 0.004 and DG > 9.98 tend to increase the radiation diversity performance and have better matching of the proposed MIMO design, respectively. The resulting gain and efficiencies including all other parameters make the proposed MIMO antenna design viable for 5G mobile terminal communications.

It is quite evident that the 3-D radiation patterns cover almost all the sides of the mobile PCB terminal. Its evident from the patterns that the identical polarized elements show identical performances. The simulated and measured polar patterns for the two adjacent antenna elements at 3 GHz frequency are shown in Fig. 12. The patterns show better results for radiation properties of the proposed design.

2.3. SAR Effects and the Impact of the User

In the given section, impacts of the user on the radiation characteristics and SAR (specific absorption rates) on the human tissues are studied. The simulated radiation characteristics of the antenna elements of proposed design are depicted in Fig. 13 in the presence of human tissues while the mobile terminal is in user-mode. The patterns seem quite efficient in the presence of the human head covering all the sides of the mobile PCB. The value of the gain parameter as well as pattern radiation coverage is good enough for 5G mobile applications. The gain values are better than 3 dBi in the presence of human tissue.

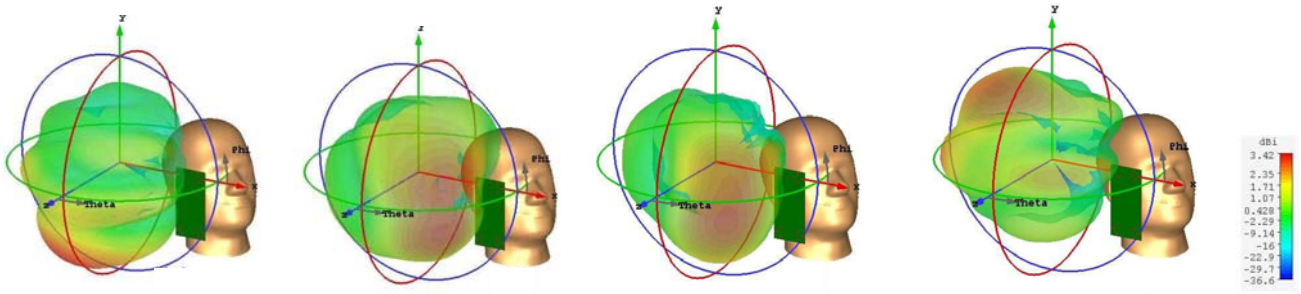

Figure 13. Simulated radiation patterns of the antenna elements showing the wider coverage while in the users talking mode, (a) Antenna-1 at 3 GHz, (b) Antenna-2 at 3 GHz, (c) Antenna-1 at 4.5 GHz, (d) Antenna-2 at 4.5 GHz.

One of the critical parametric issues for mobile terminal application is SAR. It can be defined as the function that measures the extent of absorbed electromagnetic energy by the tissues of human body while a mobile terminal transmits or receives data signals. An SAR safety guideline has been implemented to prevent the users from the harmful impacts of the EM rays. According to IEEE C95.1:2005, the safety limit to SAR has been set to '2' W/kg per 10 g of biological human tissue. The SAR values need to be very low as much as possible [28] for minimized harmful effects on the human body while a mobile device is used. The SAR limits greater than 2 are considered to be very harmful for human body. The SAR absorption by the tissues can vary by certain factors which mainly include the nature of the substrate between the device and the user, exposure to the frequency, and the geometry of the source [30]. This impact of the electromagnetic waves has increased the need for the design of the antennas with lower SAR values. The proposed design is analyzed for the SAR effects, and the simulated SAR values are shown in Fig. 14 for the four resonator MIMO antenna design at 3 GHz and 4.5 GHz frequencies, respectively. It is clear from the figure that the SAR values are very low in terms

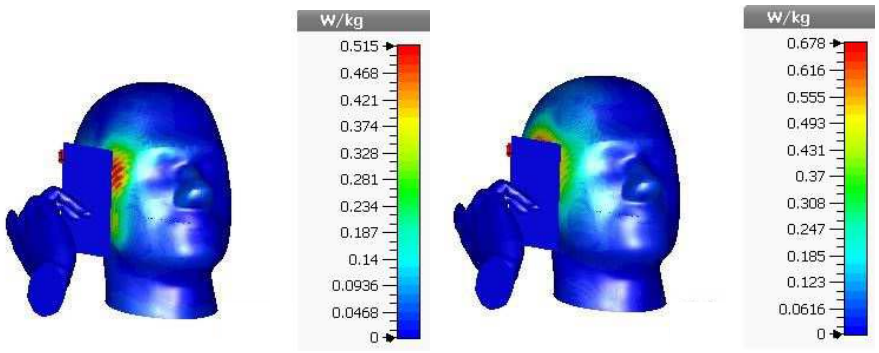

Figure 14. Simulated values of SAR in the vicinity of users head and hand for the proposed MIMO antenna design, (a) at 3 GHz, (b) at 4.5 GHz.

Table 1. Comparison of the parameters for proposed 5G MIMO antenna with respect to already reported MIMO 5G designs.

Ref. Antenna Description	BW (GHz)	η (%)	Size (mm^2)	ECC	SAR
8 & 16 element Array [17]	3.4–3.6	35–50	150×75	< 0.40	-
8-element CPW fed [22]	3.3–4.4	65–80	150×75	< 0.005	2.1
8-element square ring slot [23]	3.45–3.8	73–76	150×75	<-	1.45
8-element diamond slot [24]	3.3–3.9	60–80	150×75	< 0.01	-
4 & 8 element orthogonal MIMO [31]	3.4–3.6	50–70	150×73	< 0.07	-
Metasurface enabled antenna [32]	0.9	-	62×42	-	1.32
CPW fed with CS-EBG [33]	0.9	67	66×71	-	1.35
Dual polarized MIMO Array [34]	3.55–3.65	52–76	150×75	< 0.01	-
8-port antenna Array [35]	2.55–2.68	48–63	136×68	< 0.15	-
8-port MIMO Array with SRR	2.73–3.12 4.32–4.68	75–80	150×70	< 0.004	0.5

'η' represents the efficiency parameter.

for the safe application of mobile device by the humans.

Table 1 displays the overall comparison of the proposed 5G MIMO antenna design with some of the previously designed 5G antennas. In [22] a CPW-fed MIMO antenna is designed for 3.4–4.4 GHz operating band with an isolation of less than −16 dB among elements and 2.1 as the SAR limit. A multi-band MIMO with an isolation factor around −17 dB between antenna elements and SAR limit around 1.45 with respect to user talk mode analysis has been given in [23]. [24] presents a 5G MIMO antenna with an impedance bandwidth of 3.2–4 GHz providing an isolation of less than −17 dB along with ECC < 0.01. In comparison to almost all the reported antennas, the proposed design shows a double band operation with comparatively wider bandwidths, better efficiency, and most importantly very low correlation coefficient with high isolation between antenna elements. The isolation in the proposed MIMO design is greater than 21 dB for the entire two operating bands having ECC $\ll 0.004$ and the SAR value of 0.5 which is considered to be very safe in terms of user applications.

3. CONCLUSION

A double-polarized annular slot antenna for sub-6 GHz 5G MIMO applications has been proposed in the manuscript. The proposed MIMO antenna has annular slot antenna radiators placed along the corners of the mobile terminals. The square SRRs are placed transversely from the top side of the substrate along the slotted radiators to get the improved isolation among the elements of MIMO. By using the SRR structures, there has been a significant reduction in the mutual coupling. The resulting isolation between the elements is greater than 21 dB which is considered quite appreciable. In the proposed design, a good amount of radiation coverage with the dual-polarization is achieved on both sides of the mobile PCB. The proposed design offers the well defined characteristics for the operating frequency bands of 2.73–3.12 GHz and 4.32–4.68 GHz, respectively, with ECC < 0.004, DG > 9.98, and reliable efficiencies of more than 80 percent. The extremely low value of SAR has made the proposed design very reliable in terms of safe handling of the mobile users. All the resulting parameters can make the design a viable candidate for sub-6 GHz 5G wireless MIMO mobile applications.

REFERENCES

1. Wang, T., G. Li, J. Ding, Q. Miao, J. Li, and Y. Wang, "5G spectrum: Is China ready?," *IEEE Communications Magazine*, Vol. 53, No. 7, 58–65, 2015.

2. Li, Y., H. Zou, M. Wang, M. Peng, and G. Yang, "Eight-element MIMO antenna array for 5G/sub-6 GHz indoor micro wireless access points," *2018 International Workshop on Antenna Technology (iWAT)*, 1–4, 2018.
3. Ahmad, A., "Design and performance analysis of six element MIMO antenna for wireless routers," *2016 19th International Multi-Topic Conference (INMIC)*, 1–4, 2016.
4. Ren, Z. and A. Zhao, "Dual-band MIMO antenna with compact self-decoupled antenna pairs for 5G mobile applications," *IEEE Access*, Vol. 7, 82 288–82 296, 2019.
5. Ojaroudi Parchin, N., H. J. Basherlou, Y. I. A. Al-Yasir, A. M. Abdulkhaleq, R. A. Abd-Alhameed, and P. S. Excell, "Eight-port MIMO antenna system for 2.6 GHz LTE cellular communications," *Progress In Electromagnetics Research C*, Vol. 99, 49–59, 2020.
6. Ojaroudi Parchin, N., H. J. Basherlou, and R. A. Abd-Alhameed, "Dual circularly polarized crescent-shaped slot antenna for 5G front-end systems," *Progress In Electromagnetics Research Letters*, Vol. 91, 41–48, 2020.
7. Masoodi, I. S., I. Ishteyaq, K. Muzaffar, and M. Idrees Magray, "Low cost substrate based compact antennas for 4G/5G side-edge panel smartphone applications," *Progress In Electromagnetics Research Letters*, Vol. 91, 145–152, 2020.
8. Sarkar, D. and K. V. Srivastava, "Four element dual-band sub-6 GHz 5G MIMO antenna using SRR-loaded slot-loops," *2018 5th IEEE Uttar Pradesh Section International Conference on Electrical, Electronics and Computer Engineering (UPCON)*, 1–5, 2018.
9. Huang, B., W. Lin, J. Huang, J. Zhang, G. Zhang, and F. Wu, "A patch/dipole hybrid-mode antenna for sub-6 GHz communication," *Sensors*, Vol. 19, No. 6, 1358, 2019.
10. Li, Y., Y. Luo, G. Yang, et al., "Multiband 10-antenna array for sub-6 GHz MIMO applications in 5-G smartphones," *IEEE Access*, Vol. 6, 28 041–28 053, 2018.
11. Paul, P. M., K. Kandasamy, and M. S. Sharawi, "A multi-band U-strip and SRR loaded slot antenna with circular polarization characteristics," *Advanced Electromagnetics*, Vol. 9, No. 1, 41–48, 2020. [Online]. Available: 10.7716/aem.v9i1.1183.
12. Reshadatmand, M., H. R. Hassani, and S. M. A. Nezhad, "A compact wideband dielectric loaded H-plane sectoral ridged SIW horn antenna," *Advanced Electromagnetics*, Vol. 9, No. 2, 1–6, 2020. [Online]. Available: 10.7716/aem.v9i3.1268.
13. Deng, J., J. Li, L. Zhao, and L. Guo, "A dual-band inverted-F MIMO antenna with enhanced isolation for WLAN applications," *IEEE Antennas and Wireless Propagation Letters*, Vol. 16, 2270–2273, 2017.
14. Wong, K., C. Tsai, and J. Lu, "Two asymmetrically mirrored gap-coupled loop antennas as a compact building block for eight-antenna MIMO array in the future smartphone," *IEEE Transactions on Antennas and Propagation*, Vol. 65, No. 4, 1765–1778, 2017.
15. Ling, X. and R. Li, "A novel dual-band MIMO antenna array with low mutual coupling for portable wireless devices," *IEEE Antennas and Wireless Propagation Letters*, Vol. 10, 1039–1042, 2011.
16. Wang, Y. and Z. Du, "A wideband printed dual-antenna with a protruded ground for mobile terminals," *2014 IEEE Antennas and Propagation Society International Symposium (APSURSI)*, 1133–1134, 2014.
17. Wong, K.-L., J.-Y. Lu, L.-Y. Chen, W.-Y. Li, and Y.-L. Ban, "8-antenna and 16-antenna arrays using the quad-antenna linear array as a building block for the 3.5-GHz LTE MIMO operation in the smartphone," *Microwave and Optical Technology Letters*, Vol. 58, No. 1, 174–181, 2016. [Online]. Available: https://onlinelibrary.wiley.com/doi/abs/10.1002/mop.29527.
18. Ishteyaq, I., I. S. Masoodi, and K. Muzaffar, "Wideband printed quasi-yagi MIMO antenna for millimeter wave applications," *2019 IEEE Indian Conference on Antennas and Propagation (InCAP)*, 1–4, Dec. 2019. [Online]. Available: 1109/InCAP47789.2019.9134583.
19. Nazeri, A., A. Abdolali, and M. Mehdi, "An extremely safe low-SAR antenna with study of its electromagnetic biological effects on human head," *Wireless Personal Communications*, Vol. 109, No. 2, 1449–1462, 2019. [Online]. Available: 1007/s11277-019-06621-6.

20. Fields, R. F. E., "Ieee standard for safety levels with respect to human exposure to radio frequency electromagnetic fields, kHz to 300 GHz," *IEEE Standard*, Vol. C95.1, 2005.
21. Ojaroudi Parchin, N., Y. I. Al-Yasir, H. J. Basherlou, A. M. Abdulkhaleq, M. Sajedin, R. A. Abd-Alhameed, and J. M. Noras, "Modified PIFA array design with improved bandwidth and isolation for 5G mobile handsets," *2019 IEEE 2nd 5G World Forum (5GWF)*, 199–203, IEEE, 2019. [Online]. Available: 1109/5GWF.2019.8911725.
22. Ojaroudi Parchin, N., H. Jahanbakhsh Basherlou, Y. I. Al-Yasir, A. M. Abdulkhaleq, M. Patwary, and R. A. Abd-Alhameed, "A new CPW-fed diversity antenna for MIMO 5G smartphones," *Electronics*, Vol. 9, No. 2, 261, 2020. [Online]. Available: 3390/electronics9020261.
23. Ojaroudi Parchin, N., H. Jahanbakhsh Basherlou, Y. I. Al-Yasir, A. Ullah, R. A. Abd-Alhameed, and J. M. Noras, "Multi-band MIMO antenna design with user-impact investigation for 4G and 5G mobile terminals," *Sensors*, Vol. 19, No. 3, 456, 2019. [Online]. Available: 3390/s19030456.
24. Ojaroudi Parchin, N., H. Jahanbakhsh Basherlou, M. Alibakhshikenari, Y. Ojaroudi Parchin, Y. I. Al-Yasir, R. A. Abd-Alhameed, and E. Limiti, "Mobile-phone antenna array with diamond-ring slot elements for 5G massive MIMO systems," *Electronics*, Vol. 8, No. 5, 521, 2019. [Online]. Available: 3390/electronics8050521.
25. Ishteyaq, I., I. S. Masoodi, and K. Muzaffar, "A compact double-band planar printed slot antenna for sub-6 GHz 5G wireless applications," *International Journal of Microwave and Wireless Technologies*, 1–9, 2020. [Online]. Available: 1017/S1759078720001269.
26. Azeez, H. I., H.-C. Yang, and W.-S. Chen, "Wearable triband E-shaped dipole antenna with low SAR for IoT applications," *Electronics*, Vol. 8, No. 6, 665, 2019. [Online]. Available: 3390/electronics8060665.
27. Ren, Z., A. Zhao, and S. Wu, "MIMO antenna with compact decoupled antenna pairs for 5G mobile terminals," *IEEE Antennas and Wireless Propagation Letters*, Vol. 18, No. 7, 1367–1371, 2019.
28. Ojaroudi Parchin, N., Y. I. A. Al-Yasir, A. H. Ali, I. Elfergani, J. M. Noras, J. Rodriguez, and R. A. Abd-Alhameed, "Eight-element dual-polarized MIMO slot antenna system for 5G smartphone applications," *IEEE Access*, Vol. 7, 15 612–15 622, 2019.
29. Elshirkasi, A. M., A. Abdullah Al-Hadi, M. F. Mansor, R. Khan, and P. J. Soh, "Envelope correlation coefficient of a two-port MIMO terminal antenna under uniform and gaussian angular power spectrum with user's hand effect," *Progress In Electromagnetics Research C*, Vol. 92, 123–136, 2019.
30. Anguera, J., A. Andújar, M.-C. Huynh, C. Orlenius, C. Picher, and C. Puente, "Advances in antenna technology for wireless handheld devices," *International Journal of Antennas and Propagation*, Vol. 2013, 2013.
31. Sun, L., H. Feng, Y. Li, and Z. Zhang, "Compact 5G MIMO mobile phone antennas with tightly arranged orthogonal-mode pairs," *IEEE Transactions on Antennas and Propagation*, Vol. 66, No. 11, 6364–6369, 2018.
32. Jiang, Z. H., D. E. Brocker, P. E. Sieber, and D. H. Werner, "A compact, low-profile metasurface-enabled antenna for wearable medical body-area network devices," *IEEE Transactions on Antennas and Propagation*, Vol. 62, No. 8, 4021–4030, 2014.
33. Islam, M., M. Alam, N. Misran, M. Ismail, and B. Yatim, "Development of high gain multiband antenna with centre-offset copper strip-based periodic structure," *Microwave and Optical Technology Letters*, Vol. 57, No. 7, 1608–1614, 2015.
34. Ojaroudi Parchin, N., Y. I. Al-Yasir, J. M. Noras, and R. A. Abd-Alhameed, "Dual-polarized MIMO antenna array design using miniaturized self-complementary structures for 5G smartphone applications," *2019 13th European Conference on Antennas and Propagation (EuCAP)*, 1–4, IEEE, 2019.
35. Li, M., Z. Xu, Y. Ban, Q. Yang, and Q. Zhou, "Eight-port dual-polarized MIMO antenna for 5G smartphone applications," *2016 IEEE 5th Asia-Pacific Conference on Antennas and Propagation (APCAP)*, 195–196, 2016.